Article:

Jia, Chao, Luo, Jiewen, Fan, Jiajun orcid.org/0000-0003-3721-5745 et al. (3 more authors) (2021) Urgently reveal longly hidden toxicant in a familiar fabrication process of biomass-derived environment carbon material. Journal of Environmental Sciences (China). pp. 250-256. ISSN 1878-7320

https://doi.org/10.1016/j.jes.2020.08.001

Urgently reveal longly hidden toxicant in a familiar fabrication process of biomass-derived environment carbon material

Chao Jia[1], Jiewen Luo[1], Jiajun Fan[2], James H. Clark[1,2], Shicheng Zhang[1,3,4], Xiangdong Zhu[1,3,4,*]

1. Shanghai Key Laboratory of Atmospheric Particle Pollution and Prevention (LAP3), Department of Environmental Science and Engineering, Fudan University, Shanghai 200433, China
2. Green Chemistry Centre of Excellence, Department of Chemistry, University of York, York YO10 5DD, UK
3. Shanghai Institute of Pollution Control and Ecological Security, Shanghai 200092, China
4. Shanghai Technical Service Platform for Pollution Control and Resource Utilization of Organic Wastes, Shanghai 200438, China

Abstract: Biomass-derived N-doped carbon (BNC) is an important environmental material and widely used in the fields of water purification and soil remediation. However, the toxicant in the commonly used synthesis process of BNC materials have been largely ignored. Herein, we firstly report the presence of a highly toxic by-product (KCN) in the activation process of BNC materials consequential of the carbothermal reduction reaction. Because this carbothermal reduction reaction also regulates the N-doping and pore development of BNC materials, the KCN content directly relates with the properties of BNC material properties. Accordingly, a high KCN content (~ 611 mg) can occur in the production process of per g BNC material with high specific surface area (~ 3,600 m^2/g). Because the application performance of BNC material is determined by the surface area and available N doping, therefore, production of a BNC material with high performance entails high risk. Undoubtedly, this study proves a completely new risk recognition on a familiar

synthesis process of biomass-based material. And, strict protective device should be taken in fabrication process of biomass-derived carbon material.

Keywords:

Biomass

Biomass based N-doped carbon

Carbothermal reduction reaction

Pore

Toxic by-product

---

* Corresponding author. E-mail: zxdjewett@fudan.edu.cn (Xiangdong Zhu)

36 **Introduction**

37 Biomass-derived N-doped carbon (BNC) materials with high surface area and effective N content
38 alongside their low price and easy synthesis have encouraged applications in many fields including
39 water purification, soil remediation and energy storage (Sun et al., 2019; Tian et al., 2017; Wei et
40 al., 2019). BNC materials are usually fabricated by cooperative activation of a porogen (such as
41 $K_2C_2O_4$ or K_2CO_3) and N-dopant (such as urea or melamine) (Liu et al., 2016a; Yue et al., 2018;
42 Zhu et al., 2017b, 2018). In this universal synthetic strategy, an N-containing metal oxide (e.g.,
43 KOCN) can be firstly produced via the interaction between porogen and N-dopant, and then
44 KOCN can be further reduced by the carbon matrix (KOCN + C → KCN + CO) to enlarge pores
45 of BNC material (Luo et al., 2019; Tsubouchi et al., 2016). Remarkably, a highly toxic by-product
46 (KCN) can be formed simultaneously during this synthesis of BNC materials (Cai et al., 2015;
47 Chan et al., 2010). It should be noted that this BNC materials can be easily dispersed as dust in its
48 production plant, undoubtedly, this will pose a high risk to practitioner of BNC material production
49 (Sahu et al., 2014; Sigmund et al., 2017). In addition, while materials can be washed to remove
50 inorganic salts before their application (Liu et al., 2016b; Qian et al., 2014; Zhu et al., 2017a), the
51 associated KCN can easily be transformed to inhalable highly toxic (HCN) seriously damaging
52 the quality of the ambient environment (Kyoseva et al., 2009). With the above discussion, there
53 are great risks in the synthesis of BNC materials with this universal method. However, this risk in
54 synthesis process of BNC materials remains less understood. Revealing synthetic risk of BNC
55 material is conducive to reducing the related environmental problem, and promoting a sustainable
56 route for its large-scale production.

57 Previous studies have shown that surface area and the N doping of BNC materials can be
58 regulated by the aforementioned carbothermal reduction (KOCN + C → KCN + CO), and CO gas
59 is the main factor behind the pore increase of the material (Luo et al., 2019; Zhu et al., 2015).
60 Obviously, high CO yield can be observed during the activation process of BNC material with high
61 surface area. In addition, the mole numbers of KCN and CO produced in this reaction is the same,

62 therefore, it can be deduced that a high KCN yield can be expected in the activation process for
63 BNC materials with high surface area. In addition, their application performance (such as
64 adsorption ability and energy storage capacity) of BNC materials are mainly determined by their
65 surface area (Li et al., 2014; Ma et al., 2017; Zhu et al., 2016). Overall we can soundly inferred
66 that production of BNC materials with high performance will inevitably incur greater production
67 risks. However, in order to directly verify the above speculations, more work is still required. For
68 example, it is unclear that how much KCN can be formed during the synthetic process of BCN
69 materials, and the correlation between KCN content and the properties of BNCs also need to be
70 verified.

71 To address these gaps in knowledge, BNC materials were fabricated by co-activation of porogen
72 and N-dopant under different activation conditions through a universal fabrication method. The
73 formed KCN in the material synthesis process was quantitatively analyzed and then correlated
74 with the properties of the BNC materials, in order to illustrate which BNC material will entail high
75 synthetic risk.

76

77 **1. Materials and methods**

78 **1.1. Fabrication of biomass-derived N-doped carbon material**

79 Biomass-derived N-doped carbon (BNC) materials was prepared with a mixture of $K_2C_2O_4$,
80 melamine and biomass (80 mesh) at 700°C for 1 hr under an N_2 flow of 100 mL/min at a heating
81 rate of 5°C/min. The loading contents of $K_2C_2O_4$ and melamine were changed to explore the
82 relationship between the formation of KCN content and specific surface area of BNC materials. In
83 addition, the N-dopant plays an important role in promoting the complexation reaction to produce
84 KOCN and initiating subsequent carbothermal reduction reaction, therefore, various nitrogen
85 source including melamine, cyanuric acid, dicyandiamide, urea, *s*-triazine were used to fabricate
86 the BNC materials at 700°C with a $K_2C_2O_4$/ N-dopant /biomass weight ratio of 2:(2/3):1. Finally,
87 to remove inorganic salts, the carbonized samples were successively washed on the fume hood

88 with 2 mol/L HCl and water until a neutral pH was achieved. Samples were then dried at 100°C
89 overnight and filtered through a 100-mesh sieve.
90
91 **1.2. Characterization of biomass-derived N-doped carbon materials**
92 Cyanide anion (CN^-) in unwashed BNC material was extracted using 100 mL NaOH solution (10^-
93 ^{3} mol/L) with 30 min ultrasonic. The supernatant containing CN^- was then measured using an ion
94 meter (PXSJ-226, Inesa instrument, China) with a cyanide electrode (PXSJ-226, Inesa instrument,
95 China) at 25°C. The saturated potassium chloride electrode served as the reference electrodes.
96 Three samples (biomass, $K_2C_2O_4$ with N-dopant, and biomass mixed with $K_2C_2O_4$ and N-dopant)
97 were analyzed via online thermogravimetry–mass spectrometry (TG209F1, Netzsch, Germany) to
98 discern the CO release characteristics. The samples were heated from 25 to 900°C at a rate of
99 5°C/min in argon atmosphere. The CO release curve at low temperatures (peak 1) was produced
100 from the thermal cracking of biomass and melamine, that at medium temperatures (peak 2) was
101 produced from the decomposition of un-complexed $K_2C_2O_4$ to produce K_2CO_3 ($K_2C_2O_4 \rightarrow K_2CO_3$
102 $+ CO$), and that at high temperatures (peak 3) was produced by the carbothermal reduction reaction
103 between KOCN and the carbon matrix ($KOCN + C \rightarrow KCN + CO$).
104 Furthermore, CO gas released during the synthesis of BNC materials was semi-quantitatively
105 determined via online mass spectrometry (QIC-20, Hiden, British) with Ar atmosphere. The mass-
106 to-charge ratio value was set to 28 for CO analysis. Before the pyrolytic gas entered the online
107 mass spectrometer, the pyrolysis oil was removed with ethanol solution and cooling of solid CO_2.
108 Powder X-ray diffraction (XRD) analysis of the unwashed BNC material was performed to
109 observe the formation of KCN using a system (X'Pert PRO, Nalytical, Netherlands) to produce
110 Cu $K\alpha$ radiation at 40 kV, 40 mA in the 2θ range of 10-90°.
111 Details of the BNC material characterization methods, such as elemental compositions (C/H/N),
112 N_2 adsorption isotherm for porosity analysis and X-ray photoelectron spectroscopy (XPS) for N
113 functional groups are expounded in our previous work (Qian et al., 2016; Zhu et al., 2017c).

114 **1.3. Bisphenol A adsorption onto biomass-derived N-doped carbon materials**

115 Batch adsorption experiments were initiated after dispersion of 2.5 mg BNC materials in 25 mL
116 bisphenol A (BPA) solution with different initial concentrations (2-120 mg/L). The mixed solution
117 was shaken at 25°C with 150 r/min. After adsorption equilibrium had been reached, the supernatant
118 was filtrated by polytetrafluoroethylene membrane. The resultant BPA concentration was then
119 measured by a UV-visible spectrometer (CARY 300, Agilent, USA) at 280 nm absorbance.

120

121 **2. Results and discussion**

122 **2.1 Influence of porogen load ratio on formation of KCN**

123 The effect of the porogen ($K_2C_2O_4$) load ratio on the formation of KCN during the synthesis
124 process of BNC material was firstly considered. As shown in **Fig. 1a**, the presence of KCN can be
125 clearly confirmed by XRD pattern of unwashed BNC materials. Previous studies indicated that the
126 KOCN produced by reaction between the porogen and N-dopant was crucial for initiating the
127 subsequent carbothermal reaction (KOCN + C → KCN + CO) (Tsubouchi et al., 2016). Therefore,
128 with an increase of the $K_2C_2O_4$ load ratio, the KCN signals gradually strengthened, while the signal
129 for KOCN showed the opposite trend. And the decreased pyridinic N in BNC materials suggested
130 that $K_2C_2O_4$ was mainly complexed with pyridinic N (the pyrolysis product of N-dopant, melamine)
131 to product KOCN, which can be explained by the changes of XPS spectra (**Fig. 1b**) (Chen et al.,
132 2012; Wei et al., 2013). Accordingly, the KCN concentration increased with increasing porogen
133 loading content in unwashed BNC materials (**Fig. 1c**), which can be further confirmed by the
134 enhanced carbothermal reduction reaction between KOCN and the carbon matrix (KOCN + C →
135 KCN + CO). It is worth noting that the CO production (peak 3) also shown the same trend (**Fig.
136 1d**), further indicating an enhanced KCN in unwashed BNC materials. The decreased yield and N
137 content of BNC materials can further confirm the enhanced CO yield (Appendix A **Fig. S1a**),
138 because this studied carbothermal reduction reaction consumed carbon matrix and the organic N
139 of BNC material. Further, it should be clarified that the CO release curve at low temperatures (peak

140 1) was mainly produced from the thermal cracking of biomass and N-dopant (melamine), the CO
141 released at medium temperatures (peak 2) was mainly produced from the decomposition of un-
142 complexed $K_2C_2O_4$ to produce K_2CO_3 ($K_2C_2O_4 \rightarrow K_2CO_3 + CO$) (Appendix A **Fig. S1b**).
143 As shown in **Fig. 1c**, when the ratio between porogen and biomass was increased to 2,
144 production of per g BNC material will simultaneously generate 611 mg KCN. In addition, it has
145 been well reported that the CO produced from the carbothermal reduction reaction is the main
146 factor for the pore enlargement of BNC material (Luo et al., 2019), as verified by the strongly
147 positive relationship between the CO in peak 3 and the Brunauer-Emmett-Teller (BET) surface
148 area (R^2 = 0.91, **Fig. 1e**). Based on the stoichiometry of the carbothermal reduction reaction, the
149 mole number of KCN and CO are the same. Therefore, it is reasonable that a strongly positive
150 correlation can be observed between the KCN concentration and BET surface area of BNC
151 materials (R^2 = 0.86, **Fig. 1e**). In conclusion, the production of BNC materials with high BET
152 surface area will simultaneously generate great toxicant and risk, as indicated in **Fig. 2**.
153
154 **2.2. Influence of melamine load ratio on formation of KCN**
155 The effect of melamine (as the source of N doping) on the KCN content in BCN materials was
156 also studied. As shown in **Fig. 3a**, KCN content was significantly increased with melamine content,
157 as confirmed by the enhanced KCN signals in the XRD patterns (Appendix A **Fig. S2a**). When the
158 weight ratio between the N-dopant and biomass was increased to 1, production of per g BNC
159 material will simultaneously generate 328 mg KCN. In addition, CO production (peak 2) decreased
160 with increasing melamine loading, indicating an enhanced complexation reaction between $K_2C_2O_4$
161 and melamine to form KOCN (**Fig. 3b**). Therefore, the progress of the carbothermal reduction
162 reaction between KOCN and the carbon matrix to produce KCN and CO was enhanced, which can
163 be verified by the high yield of CO in peak 3 and strong KCN signals in XRD patterns (**Fig. 3b**
164 **and** Appendix A **Fig. S2a**). In addition, the continuously decreased yield of BNC materials can
165 further confirm the enhanced CO yield in peak 3 (Appendix A **Fig. S2b**), as an evidence of studied

166 carbothermal reduction reaction was a process that consumed carbon matrix to produce the same
167 mole number of CO and KCN. As mentioned above, the growth in porosity of BNC materials can
168 be indicated by the yield of CO in peak 3. Accordingly, it is reasonable to assume that the
169 production of BNC materials with high surface area will inevitably generate a substantial amount
170 of highly hazardous by-product (KCN).
171
172 **2.3. Influence of N-dopant type on formation of KCN**
173 The type of N-dopant also plays an important role in promoting the complexation reaction to
174 produce KOCN and initiating subsequent a carbothermal reduction reaction. As shown in
175 Appendix A **Fig. S3a**, great differences can be observed in the XRD patterns of BNC materials
176 derived from different N-dopants. High quality data for KCN signals were present in the unwashed
177 BNC material derived from melamine, while the *s*-triazine-activated BNC material mainly showed
178 strong K_2CO_3 signals in the XRD patterns. This result may be caused by the different strengths of
179 carbothermal reduction reactions during the synthesis process of BNC materials, which can be
180 strongly implied by the CO in peak 3 (**Fig. 3c**). Accordingly, melamine-activated BNC material
181 had a relatively strong CO yield (peak 3) during its synthesis process, while *s*-triazine-activated
182 BNC material had a weaker CO yield in peak 3 (**Fig. 3c**). It should be noted that a low-boiling
183 point N-dopant can be largely volatilized in the low temperature range, resulting in a low
184 complexation ability with the porogen to form KOCN.
185 This can further weaken the carbothermal reduction reaction between KOCN and carbon matrix
186 to produce KCN and CO, as confirmed by a strong positive relationship (R^2 = 0.95) between the
187 boiling point of N-dopant and the CO in peak 3 (**Fig. 3d**). Therefore, it is reasonable to assume
188 that high-boiling point N-dopant activated-BNC material gives a high BET surface area, as
189 indicated by the stronger CO (peak 3) yield (Appendix A **Fig. S3b**). As KCN and CO will be
190 formed in the same molar quantities, so it can be deduced that BNC material activated by high
191 boiling point N-dopants are likely to be associated with more KCN formation during the synthesis

process.

2.4. Disclose high risk from a biomass-derived N-doped carbon material with high performance

BPA was selected as a common organic pollutant to firstly verify the relationship between basic properties (such as surface area and N content) of BNC materials and its application performance (Chu et al., 2019; Xiao et al., 2018). And the adsorption isotherms of BNC materials were fitted to the Langmuir models (Li et al., 2018; Mian et al., 2019). As shown in Appendix A **Fig. S4**, as-prepared BNC materials exhibited high BPA adsorption capacity (maximum 938 mg/g) and adsorption rate, obvious higher than reported materials (Arampatzidou et al., 2018; Arampatzidou and Deliyanni, 2016; Jin et al., 2018, 2015; Zhang et al., 2010). Moreover, the maximum BPA adsorption capacity of BNC material ranged from 132 to 938 mg/g because of the significant differences in surface area and N content (Appendix A **Table S1**). Generally, BPA adsorption capacity increased with increasing BET surface area of the BNC material (**Fig. 4a**), confirming the inclusion function of BNC pores on organic pollutant immobilization via strong π-π bonds (Bhatnagar and Anastopoulos, 2017; Zuo et al., 2016). In addition, BPA adsorption capacity per surface area (q_{BET}) for BNC materials was further studied to clarify the contribution of N-doping to BPA adsorption. As shown in **Fig. 4b**, the q_{BET} of some BNC materials was generally higher than that porous carbon material (a material without N doping), indicating a positive role of N-doping in BPA adsorption. Therefore, it can be concluded that high BPA adsorption capacity is mainly linked to BNC materials with high BET surface areas, but available N-doping can further enhance their BPA adsorption capacity. Moreover, the above studies indicate that BNC materials with high specific surface area will be associated with high KCN content formation. Therefore, it is a reasonable to infer that fabrication of BNC material with high adsorption performance will generate high risk during its synthesis progress.

3. Conclusions

In summary, a highly toxic by-product (KCN) was firstly observed in a common synthesis process of BNC material, which was strongly affected by activation conditions, such as the loading ratio and type of porogen and N-dopant. Meanwhile, BNC material with high BET surface area will associate high KCN content formation. And, ~ 611 mg KCN can be found in the synthesis process of per g BNC material with high surface area (~ 3,600 m^2/g). Because the determining factor in the ability of BNC materials to adsorb organic pollutant is its surface area, the fabrication of BNC material with high adsorption performance will generate more KCN. This important discovery must be taken into account in the synthesis and application of BNC materials.

Declaration of competing interest

The authors declare that they have no known competing financial interests or personal relationships that could have appeared to influence the work reported in this paper.

Acknowledgments

This work was supported by the National Natural Science Foundation of China (No. 21876030).

Appendix A. Supplementary data

Supplementary data associated with this article can be found in the online version at xxxxxx.

References

Arampatzidou, A., Voutsa, D., Deliyanni, E., 2018. Removal of bisphenol A by Fe-impregnated activated carbons. Environ. Sci. Pollut. R. 25, 25869-25879.

Arampatzidou, A.C., Deliyanni, E.A., 2016. Comparison of activation media and pyrolysis temperature for activated carbons development by pyrolysis of potato peels for effective adsorption of endocrine disruptor bisphenol-A. J. Colloid Interface Sci. 466, 101-112.

Bhatnagar, A., Anastopoulos, I., 2017. Adsorptive removal of bisphenol A (BPA) from aqueous solution: A review. Chemosphere 168, 885-902.

Cai, Y.W., Tang, H,M,, Wang, X.G., Wang, L.Y., Zhu, H.Y., 2015. Simulation assessment of dangerous consequence caused by toxic gas products during KCN decontamination process. Adv. Mater. Res. 1092-1093, 907-911.

Chan, A., Balasubramanian, M., Blackledge, W., Mohammad, O.M., Alvarez, L., Boss, G.R., 2010. Cobinamide is superior to other treatments in a mouse model of cyanide poisoning. Clin. Toxicol. 48, 709-717.

Chen, L.F., Zhang, X.D., Liang, H.W., Kong, M., Guan, Q.F., Chen, P., 2012. Synthesis of nitrogen-doped porous carbon nanofibers as an efficient electrode material for supercapacitors. ACS Nano 6, 7092-7102.

Chu, G., Zhao, J., Liu, Y., Lang, D., Wu, M., Pan, B., 2019. The relative importance of different carbon structures in biochars to carbamazepine and bisphenol A sorption. J. Hazard. Mater. 373, 106-114.

Jin, Q., Zhang, S., Wen, T., Wang, J., Gu, P., Zhao, G., 2018. Simultaneous adsorption and oxidative degradation of Bisphenol A by zero-valent iron/iron carbide nanoparticles encapsulated in N-doped carbon matrix. Environ. Pollut. 243, 218-227.

Jin, Z., Wang, X., Sun, Y., Ai, Y., Wang, X., 2015. Adsorption of 4-n-nonylphenol and bisphenol-A on magnetic reduced graphene oxides: A combined experimental and theoretical studies. Environ. Sci. Technol. 49, 9168-9175.

Kyoseva, V., Todorova, E., Dombalov, I.,2009. Comparative assessment of the methods for destruction of cyanides used in gold mining industry. J. Univ. Chem. Techno. Metall. 44, 403-408.

Li, X., Yuan, H., Quan, X., Chen, S., You, S., 2018. Effective adsorption of sulfamethoxazole, bisphenol A and methyl orange on nanoporous carbon derived from metal-organic frameworks. J. Environ. Sci. 63, 250-259.

Li, Z., Xu, Z., Wang, H., Ding, J., Zahiri, B., Holt, C.M.B., 2014. Colossal pseudocapacitance in a high functionality–high surface area carbon anode doubles the energy of an asymmetric supercapacitor. Energ. Environ. Sci. 7, 1708-1718.

Liu, J., Deng, Y., Li, X., Wang, L., 2016a. Promising nitrogen-rich porous carbons derived from one-step calcium chloride activation of biomass-based waste for high performance supercapacitors. ACS Sustainable Chem. Eng. 4, 177-187.

Liu, W.J., Tian, K., Ling, L.L., Yu, H.Q., Jiang, H., 2016b. Use of nutrient rich hydrophytes to create N,P-dually doped porous carbon with robust energy storage performance. Environ. Sci. Technol. 50, 12421-12428.

Luo, J., Jia, C., Shen, M., Zhang, S., Zhu, X., 2019. Enhancement of adsorption and energy storage capacity of biomass-based N-doped porous carbon via cyclic carbothermal reduction triggered by nitrogen dopant. Carbon 155, 403-409.

Ma, Q., Yu, Y., Sindoro, M., Fane, A.G., Wang, R., Zhang, H., 2017. Carbon-based functional materials derived from waste for water remediation and energy storage. Adv. Mater. 29, 1605361.

Mian, M.M., Liu, G., Yousaf, B., Fu, B., Ahmed, R., Abbas, Q., 2019. One-step synthesis of N-doped metal/biochar composite using NH_3-ambiance pyrolysis for efficient degradation and mineralization of methylene blue. J. Environ. Sci. 78, 29-41.

Qian, F., Zhu, X., Liu, Y., Hao, S., Ren, Z.J., Gao, B., 2016. Synthesis, characterization and adsorption capacity of magnetic carbon composites activated by CO_2: implication for the catalytic mechanisms of iron salts. J. Mater. Chem. A. 4, 18942-18951.

Qian, W., Sun, F., Xu, Y., Qiu, L., Liu, C., Wang, S., 2014. Human hair-derived carbon flakes for electrochemical supercapacitors. Energ. Environ. Sci. 7, 379-386.

Sahu, D., Kannan, G.M., Vijayaraghavan, R., 2014. Carbon black particle exhibits size dependent toxicity in human monocytes. Int. J. Inflamm. 2014, 10.

Sigmund, G., Huber, D., Bucheli, T.D., Baumann, M., Borth, N., Guebitz, G.M., 2017. Cytotoxicity of biochar: A workplace safety concern? Environ. Sci. Technol. Lett. 4, 362-366.

Sun, B., Yuan, Y., Li, H., Li, X., Zhang, C., Guo, F., 2019. Waste-cellulose-derived porous carbon adsorbents for methyl orange removal. Chem. Eng. J. 371, 55-63.

Tian, W., Zhang, H., Sun, H., Tadé, M.O., Wang, S., 2017. Template-free synthesis of N-doped carbon with pillared-layered pores as bifunctional materials for supercapacitor and environmental applications. Carbon 118, 98-105.

Tsubouchi, N., Nishio, M., Mochizuki, Y., 2016. Role of nitrogen in pore development in activated carbon prepared by potassium carbonate activation of lignin. Appl. Surf. Sci. 371, 301-306.

Wei, J., Zhou, D., Sun, Z., Deng, Y., Xia, Y., Zhao, D., 2013. A controllable synthesis of rich nitrogen-doped ordered mesoporous carbon for CO_2 capture and supercapacitors. Adv. Func. Mater. 23, 2322-2328.

Wei, L., Zhang, Y., Chen, S., Zhu, L., Liu, X., Kong, L., 2019. Synthesis of nitrogen-doped carbon nanotubes-$FePO_4$ composite from phosphate residue and its application as effective Fenton-like catalyst for dye degradation. J. Environ. Sci. 76, 188-198.

Xiao, P., Wang, P., Li, H., Li, Q., Shi, Y., Wu, X.L., 2018. New insights into bisphenols removal by nitrogen-rich nanocarbons: Synergistic effect between adsorption and oxidative degradation. J. Hazard. Mater. 345, 123-130.

Yue, L., Xia, Q., Wang, L., Wang, L., DaCosta, H., Yang, J., 2018. CO_2 adsorption at nitrogen-doped carbons prepared by K_2CO_3 activation of urea-modified coconut shell. J. Colloid Interface Sci. 511, 259-267.

Zhang, D., Pan, B., Zhang, H., Ning, P., Xing, B., 2010. Contribution of different sulfamethoxazole species to their overall adsorption on functionalized carbon nanotubes. Environ. Sci. Technol. 44, 3806-3811.

Zhu, G., Chen, T., Hu, Y., Ma, L., Chen, R., Lv, H., 2017a. Recycling $PM_{2.5}$ carbon nanoparticles generated by diesel vehicles for supercapacitors and oxygen reduction reaction. Nano Energy 33, 229-237.

Zhu, L., Shen, F., Smith, R.L., Yan, L., Li, L., Qi, X., 2017b. Black liquor-derived porous carbons from rice straw for high-performance supercapacitors. Chem. Eng. J. 316, 770-777.

Zhu, X., Liu, Y., Qian, F., Lei, Z., Zhang, Z., Zhang, S., 2017c. Demethanation trend of hydrochar induced by organic solvent washing and its influence on hydrochar activation. Environ. Sci. Technol. 51, 10756-10764.

Zhu, X., Qian, F., Liu, Y., Matera, D., Wu, G., Zhang, S., 2016. Controllable synthesis of magnetic carbon composites with high porosity and strong acid resistance from hydrochar for efficient removal of organic pollutants: An overlooked influence. Carbon 99, 338-347.

Zhu, X., Qian, F., Liu, Y., Zhang, S., Chen, J., 2015. Environmental performances of hydrochar-derived magnetic

carbon composite affected by its carbonaceous precursor. RSC Advances 5, 60713-60722.

Zhu, Y., Chen, M., zhang, Y., Zhao, W., Wang, C., 2018. A biomass-derived nitrogen-doped porous carbon for high-energy supercapacitor. Carbon 140, 404-412.

Zuo, L., Guo, Y., Li, X., Fu, H., Qu, X., Zheng, S., 2016. Enhanced adsorption of hydroxyl- and amino-substituted aromatic chemicals to nitrogen-doped multiwall carbon nanotubes: A combined batch and theoretical calculation study. Environ. Sci. Technol. 50, 899-905.

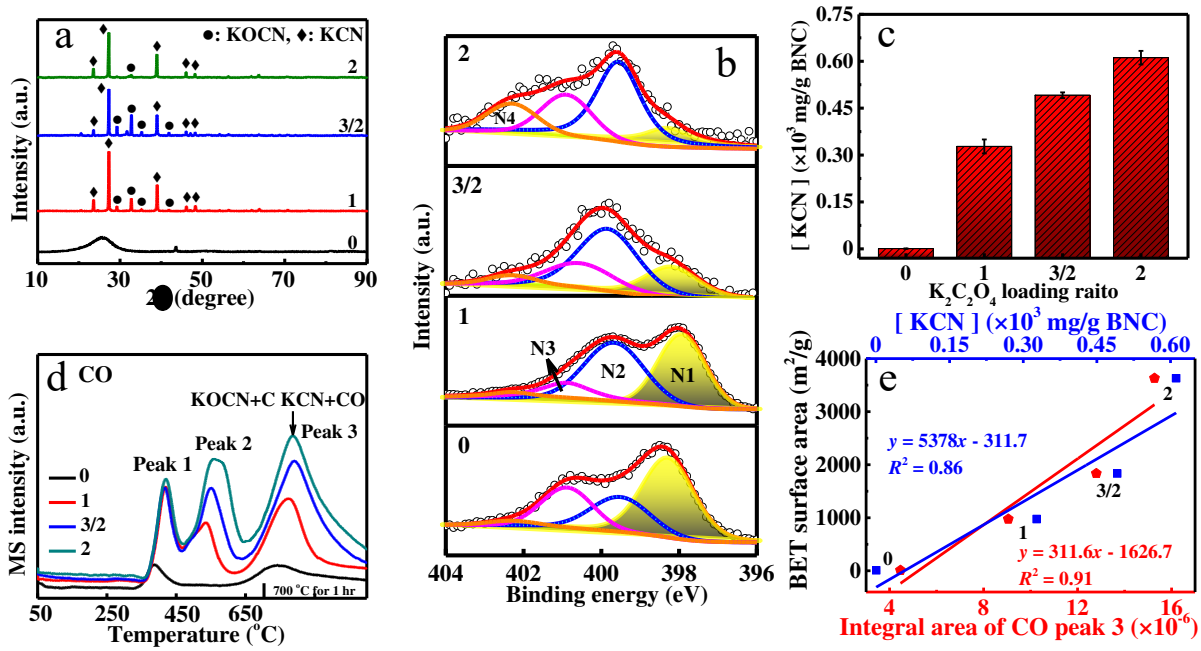

Fig. 1. (a) X-ray diffraction (XRD) pattern, (b) X-ray photoelectron spectroscopy (XPS) spectra, (c) KCN concentration ([KCN]), (d) the release of CO during the preparation process (e) linear relationship between the integral area of CO peak 3 and the Brunauer-Emmett-Teller (BET) surface area and linear relationship between the formed KCN concentration and BET surface area for biomass-derived N-doped carbon (BNC) material prepared from various $K_2C_2O_4$ loading ratios. N1: pyridinic N; N2: pyrrolic N; N3: quaternary N; N4: oxidic N; MS: mass spectroscopy.

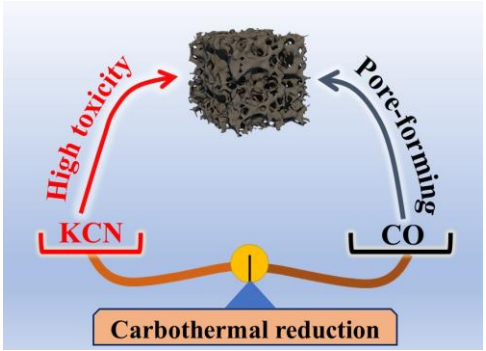

Fig. 2. Schematic diagram for the effect of carbothermal reduction reaction on pore development and KCN formation (risk) of BNC material.

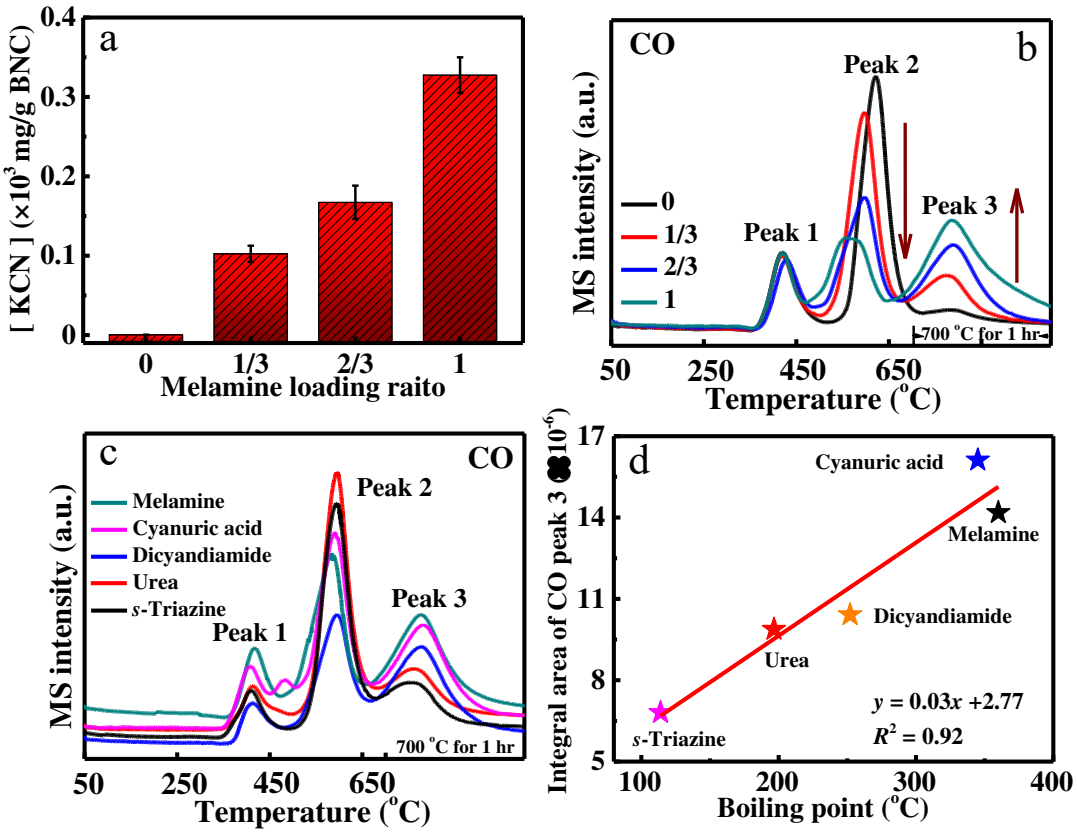

Fig. 3. (a) KCN concentration in BNC materials obtained from various melamine loading ratio, effects of (b) the melamine loading ratio and (c) N dopants on the release of CO during the preparation process of BNC materials, (d) linear correlation between boiling point of loaded N dopants and the integral area of CO peak 3 of as-prepared BNC materials.

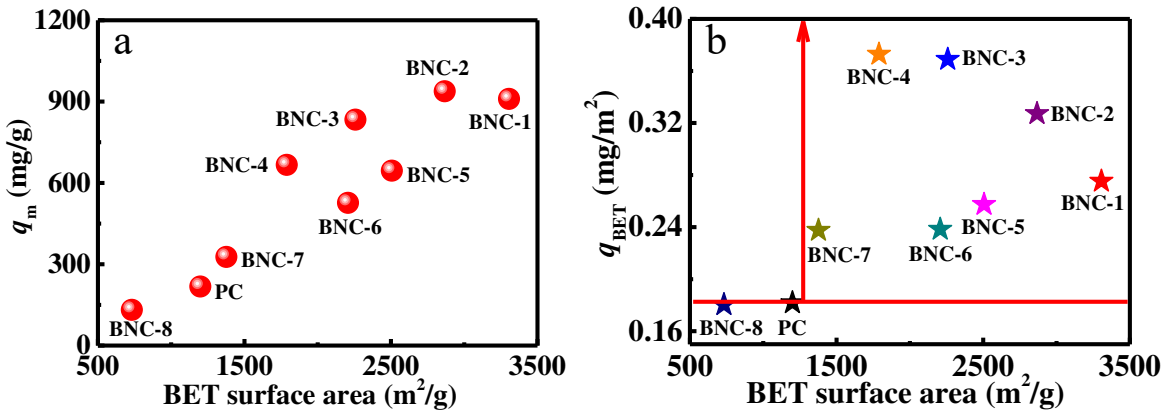

Fig. 4. (a) Relationship between BET surface area and bisphenol A (BPA) adsorption capacity of BNC materials and (b) surface area of BNC materials versus q_{BET}. $q_{BET} = q_m$/BET surface area, suggesting BPA adsorption capacity per BET surface area. q_m: the maximal adsorption capacity. PC: porous carbon material activated without N dopant. BNC-*x*: the selected BNC material with various porosity and N dope content.